Study on Monitoring of Stress and Strain during Curing Process of Fiber Metal Laminates

Xuhui Kang[1], Lihua Zhan[1, 2 *], Xintong Wu[1], Tengfei Chang[2] and Jiayang He[2]
[1]*School of Mechanical and Electrical Engineering, Central South University, Changsha, China*
[2]*Institute of Light Alloy, Central South University, Changsha, China*

Keywords: Fiber Metal Laminates; Stress and Strain Monitoring; FBG and Thermocouples; Strain Definition Method.

Abstract: Traditional metal materials and fiber reinforced composites are unable to meet the requirements of lightweight and impact resistance of aerospace components and the advent of fiber metal laminates has solved this problem. Most of the existing researches on FMLs focus on the improvement of material system and impact properties, while little attention has been paid to the changes of stress and strain during the forming process. Moreover, most of the existing monitoring methods are not suitable for non-destructive monitoring of strain during the whole forming process. In this paper, a strain monitoring method based on Fiber Bragg Grating (FBG) and Thermocouple (TC) is proposed, which can be applied to the forming process of autoclave without destroying the original stress distributions and component shapes of the parts. The strain variation process during the curing of FMLs was monitored and analyzed by using FBG+TC, so as to establish theoretical model of forming process, propose strain monitoring method based on Strain Definition (SD) and analyze comprehensively the characteristics and applicability of the three methods.

1 INTRODUCTION

Aerospace components are gradually developing towards lightweight and impact resistance, which cannot be met by traditional aerospace composites and single metals comprehensively. Fiber metal laminates have attracted more and more attention all over the world due to their primely comprehensive properties. Fiber Metal Laminates (FMLs) were first introduced and developed by Delft University of Technology in the Netherlands (Vlot and Gunnink, 2001; Vlot, 2001). It is a new type of super-hybrid composite material which is cured by alternating layers of metal sheets and fiber reinforced composites at specific temperatures and pressures (Sinmazçelik et al., 2011; Asundi and Choi, 1997), as is shown in Figure 1. FMLs, which not only possess the highly stiffness and strength of composites and the toughness and machinability of metals, but also derive specifically excellent damage tolerance and fatigue properties and impact resistance of FMLs, combine the properties of metal and fiber reinforced composites to overcome the shortcomings of single components (Vogelesang and Vlot, 2000; Aniket et al., 2016). Because of the above advantages, FMLs have been well applied to aviation. There are many theoretical and experimental studies on FMLs all over the world, such as the material system improvement (Sexton et al., 2012; Vo et al., 2013; Pan and Yapici, 2015), performance prediction like basic mechanical properties (Moussavi-Torshizi et al., 2010), low-speed impact performance (Vlot, 1996; Rubiogonzález et al., 2016; Tsartsaris et al., 2011.) and bird impact (Zhu et al., 2014), and molding methods like shot peening (Miao et al., 2010). However, the research on the stress and strain of FMLs is relatively rare, especially that of the evolution of stress and strain and the formation of residual stress in the curing process. The residual stress of FMLs is mainly formed during the curing process. The residual stress mainly results from the curing shrinkage caused by the curing reaction of the matrix resin and the thermal mismatch stress generated during the temperature history change due to the difference in the thermal expansion coefficient of the component materials. In addition, insufficient or excessive defects and pores of the resin after curing also contribute to the formation of residual stress. The excessively residual stress of FMLs not only makes for the local delamination, warping, interfacial stripping and other damage by the

Kang, X., Zhan, L., Wu, X., Chang, T. and He, J.
Study on Monitoring of Stress and Strain during Curing Process of Fiber Metal Laminates.
DOI: 10.5220/0008186301030109
In *The Second International Conference on Materials Chemistry and Environmental Protection (MEEP 2018)*, pages 103-109
ISBN: 978-989-758-360-5

interfacial stress concentration, especially for the parts of complex structure, but also situates the fiber in an unfavorable compression state, degrades the performance of the composite, and even breaks the fiber or cracks matrix.

Ghasemi A R et al. (Ghasemi et al., 2016.) utilized incremental hole drilling (IHD) method to measure the residual stress distribution of FMLs along the thickness direction. The residual stress was calculated in combination with the coefficient matrix. The theoretical value of the residual stress is calculated based on the classical laminate theory. By comparing the experimental and theoretical values, it was found that the two are well matched. The IHD method can be used to evaluate the non-uniform residual stress of the FMLs along the thickness direction. However, the IHD method will destroy the part due to drilling at the point to be measured, and because the borehole releases part of the residual stress, changing the original stress distribution. IHD method makes the shape of the part change. Abouhamzeh M et al. (Abouhamzeh et al., 2015) based on the classical laminate theory, established a theoretical expression for the FMLs curing residual stress and the warp deformation of the asymmetric layup structure by adding resin shrinkage and other corrections. Compared with the finite element simulation results, the accuracy of the model is verified.

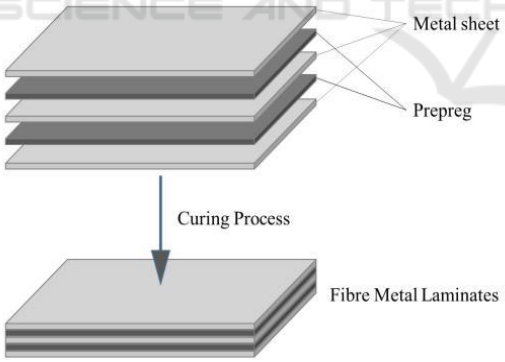

Figure 1: Fiber Metal Laminates structure.

The research on the residual stress of existing FMLs rarely centers around the evolution law of the stress of the part during the curing process, and the damage detection method has done harm to the part and changed its original stress distribution greatly. On the ground of the advantages and disadvantages of existing research, a method suitable for measuring the strain evolution of FMLs laminate curing process is proposed, namely "Fiber Bragg Grating + thermocouple (FBG + TC)" strain measurement method. This method does not damage the part and the original stress distribution of the part. The strain evolution law can be monitored throughout the curing process and even in the service phase, and reliable measurement results can be obtained. In this paper, the curing process of fiber metal laminates is firstly analyzed, and a simplified theoretical model is established. Then the FBG+TC method is used to measure the strain evolution process of FMLs during the curing process, and compared with the theoretical calculation results, the accuracy of the measurement method is confirmed. This study will lay a solid foundation for those on the stress evolution and formation of FMLs.

2 METHOD

In this paper, the theoretical solution is obtained by establishing a process theory model associated with temperature and stress. And the experimental value is measured by FBG+TC method and definition method. The stress-strain evolution process of FMLs was explored by comprehensive comparative analysis.

2.1 Materials and Instruments

The FMLs used in this experiment are made of 0.3 mm thick 2024 aluminum alloy sheet and 0.188 mm thick carbon fiber reinforced epoxy resin based T800/X850 prepreg (Cytec) alternately laminated. The size of the product is 150 mm * 50 mm. The hot-pressing process is used to cure the FMLs. The autoclave used in this experiment is an experimental YT-13-03 autoclave (Dalian Yintian) whose size is Φ650mm×1000mm. The FBG sensor and the K-type thermocouple used for monitoring separately measure the wavelength and temperature data, and the strain data are obtained by the temperature compensation method. The FBG wavelength data are collected in real time by the FBG demodulator (ZenOptics960, Shanghai), the thermocouple temperature data are collected in real time using a data recorder (TP700, Shenzhen TOPRIE). The instrument used is shown in Figure 2.

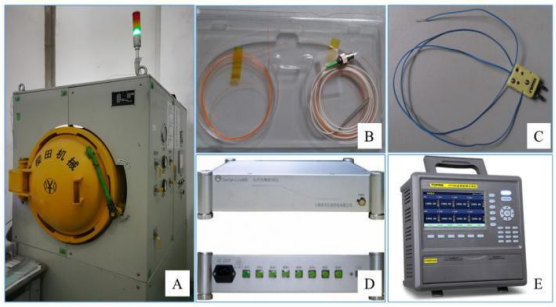

(A) Autoclave YT-13-03 (B) FBG (C) K-type thermocouple
(D) FBG Demodulator (E) Data recorder

Figure 2: Instruments for monitoring the FMLs curing process.

The instrument employed to measure the length, which is used for calculating the strain based on the definition of strain is 3D scanner (ATOS) shown in Figure 3.

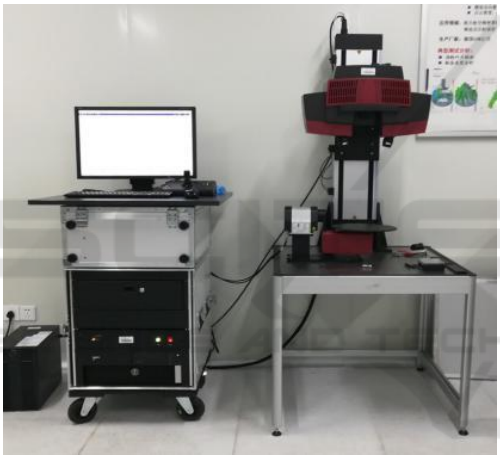

Figure 3: ATOS 3D scanner.

2.2 Method

2.2.1 Theoretical Model of Forming Process

Since the standard layups of FMLs are symmetrically layered, despite of the influence of the interface between the metal sheets and the fiber reinforced composites, the FMLs are considered to be a combination of two layers of heterogeneous materials without internal moments, as is shown in Figure 4. There are three assumptions (Oken and June, 1895):

a. The residual stress is a plane stress;

b. Symmetrical layup of the laminate, the resultant force of residual stress is zero;

c. The interface is firmly bonded, and the metal layer and the composite layer are uniformly deformed during the cooling process.

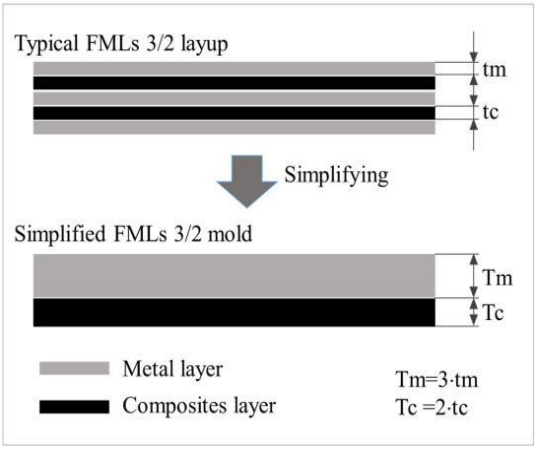

Figure 4: Simplified structure of FMLs.

Considering the same deformation, there are:

$$\begin{bmatrix} \frac{1}{E_1} & -\frac{\nu}{E_1} \\ -\frac{\nu}{E_1} & \frac{1}{E_1} \end{bmatrix} \cdot \begin{bmatrix} \sigma_{L_1} \\ \sigma_{T_1} \end{bmatrix} + \begin{bmatrix} \alpha_{L_1} \\ \alpha_{T_1} \end{bmatrix} \cdot \Delta T \tag{1}$$

$$= \begin{bmatrix} \frac{1}{E_{L2}} & -\frac{\nu_{TL}}{E_{T2}} \\ -\frac{\nu_{LT}}{E_{L2}} & \frac{1}{E_{T2}} \end{bmatrix} \cdot \begin{bmatrix} \sigma_{L_2} \\ \sigma_{T_2} \end{bmatrix} + \begin{bmatrix} \alpha_{L_2} \\ \alpha_{T_2} \end{bmatrix} \cdot \Delta T$$

E, ν, α, σ are Young's modulus, Poisson's ratio, thermal expansion coefficient and residual stress, respectively. 1 and 2 represent metals and composites, L is the composite along the fiber direction, and T is the composite material along the direction perpendicular to the fiber.

Considering that the resultant force of residual stress is zero, there are:

$$\begin{bmatrix} \sigma_{L_1} \\ \sigma_{T_1} \end{bmatrix} \cdot t_1 + \begin{bmatrix} \sigma_{L_2} \\ \sigma_{T_2} \end{bmatrix} \cdot t_2 = 0 \tag{2}$$

Where t1 is the total thickness of the metal layer and t2 is the total thickness of the composite layer.

Since the differences in thermal expansion of the composite material along the fiber direction and the metal layer are much larger than the direction of the vertical fiber, the stress distribution in the direction of the vertical fiber is ignored, and the expression of residual stress is:

$$\sigma_{L_1} = E_1 \cdot \left[1 + \frac{t_1 \cdot E_1}{t_2 \cdot E_2}\right]^{-1} \cdot (\alpha_2 - \alpha_1) \cdot \Delta T \tag{3}$$

$$\sigma_{L_2} = -\frac{t_1}{t_2} \cdot \sigma_{L_1}$$

2.2.2 FBG+TC Method

FBG is widely used in temperature, strain, and corrosion and curing of composite materials (Qiu et al., 2013; Huang, 1998; Lo and Xiao, 1998) due to its anti-electromagnetic interference, light weight, small size, and corrosion resistance (Majumder et al., 2008). However, FBG has strain-temperature cross-sensitivity problem (Dewynter-Marty et al., 1998; Farahi et al., 1990). (Majumder et al., 2008) gives a variety of temperature compensation methods to solve the cross-sensitivity scheme. Considering the advantages and disadvantages and the actual situation, this paper uses thermocouple to realize temperature compensation.

The relationship between the wavelength measured by FBG and the temperature measured by the K-type thermocouple is shown in equation (4):

$$\lambda_i - \lambda_0 = K_T(T_i - T_0) + K_\varepsilon(\varepsilon_i - \varepsilon_0) \quad (4)$$

In the formula, λ, T and ε are wavelength, temperature and strain respectively. The foot mark 0 represents the initial value, the foot mark i stands for the real-time value at time i, and K_T and K_ε are the temperature sensitivity coefficient and the strain sensitivity coefficient respectively. It is considered that the initial value of the strain is 0, and the strain calculation formula (5) can be derived from the equation (4).

$$\varepsilon_i = \frac{1}{K_\varepsilon}[(\lambda_i - \lambda_0) - K_T(T_i - T_0)] \quad (5)$$

2.2.3 Strain Definitions Method

The strain definition method is based on the definition of strain, and the surface of the part before and after the curing process are scanned with an ATOS three-dimensional scanner, moreover the original length L and the length after curing L_1 are measured from scan results, and the residual strain value is calculated by the formula (6).

$$\varepsilon = \frac{L_1 - L}{L} \quad (6)$$

2.3 Experimental Procedure

The experimental procedure shown in Figure 5 was designed to incorporate the FBG+TC method and the definition method. The surface anodizing treatment process is intended for changing the surface micromorphology of sheet metal so that the metal and the composite material are more firmly bonded, which is a necessary step towards the commercial GLARE laminate (Sinmazçelik et al., 2011; Botelho et al., 2006). Table 1 shows the stacking order of the parts. Figure 6 shows the experimental layout. Table 1 shows the layup information of the parts. The experiment is repeatedly conducted three times.

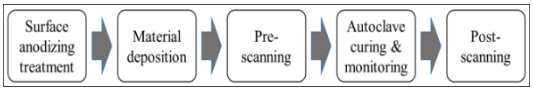

Figure 5: Experimental procedure.

Table 1: Layup information of the parts.

Sample No.	Lay-up
1	2024-T3
2	2024-T3/CFRP 0° /CFRP 0° /2024-T3

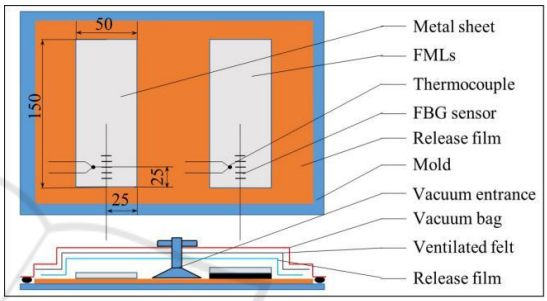

Figure 6: The experimental layout.

3 RESULTS AND ANALYSIS

The theoretical model method, FBG+TC method and definition method are used to solve the strain in the FMLs molding process. By comparing the results of the three methods, it is found that the FBG+TC method and the definition method perform better in monitoring the strain. The results are shown below.

Regarding the solution of the theoretical model, since the thermal property parameters of the material T800/X850 cannot be directly detected from the literature, it is obtained by the approximate solution method. A method for solving the equivalent thermal expansion coefficient and equivalent Young's modulus of fiber composites based on volume fraction is given by (Schapery, 1968.). By consulting the literature, the parameters contain elastic modulus (E), coefficient of thermal expansion (CTE) and volume fraction (VF) of T800 fiber and X850 resin are shown in Table 2.

Table 2: Material properties of CFRP.

Material	E_{11} (GPa)	CTE_{11} (μm/℃)	VF
T800	294	-0.56	0.65
X850	2(**)	60(***)	0.35

(** Moussavi-Torshizi et al., 2010; ***Zhang et al., 2006)

The physical properties of the composite materials T800/X850 and aluminum alloys 2024-T3 obtained by literature and calculation are shown in Table 3:

Table 3: Material properties of CFRP and 2024-T3.

Material	E_{11} (GPa)	CTE_{11} (μm/℃)	t (mm)
T800/X850	191.8	-0.339	0.376
2024-T3	72.4	23.2	0.6

The process temperature of T800/X850 is 180 °C. In order to ensure the uniformity with the experiment, the cooling temperature is 24 °C. According to the equations (3), the average stress of the aluminum alloy layer is σ_{al} = 165.917MPa, and the average stress of the composite layer is σ_{cf} = -264.762 MPa. This indicates that for the internal stress of Al-CFRP laminate, the residual tensile stress in the aluminum alloy layer is 165.917 MPa; the composite layer subjected to residual compressive stress and the size is 264.762 MPa.

The length dimensions of the parts before and after curing are scanned using an ATOS scanner. The internal stress of the aluminum alloy layer of the FMLs after compensation is obtained, which is shown in Table 4.

Table 4: Result of strain definition method.

	L1 (mm)	L2 (mm)	L3 (mm)
Uncured			
2024	149.8597	149.8627	149.8627
FMLs_1	149.7815	150.0544	150.0509
FMLs_2	149.774	150.054	150.059
FMLs_3	150.181	150.344	150.411
Cured			
2024	149.8597	149.8627	149.8627
FMLs_1	149.7815	150.0544	150.0509
FMLs_2	149.774	150.054	150.059
FMLs_3	150.181	150.344	150.411
Stress (MPa)			
2024	FMLs_1	FMLs_2	FMLs_3
50.55011	169.0378	176.3602	177.2773

The monitoring results of Group 1 using FBG+TC method is displayed in Figure 7.

The part temperature follows the air temperature in the tank, and the strain changes with temperature. Compared with the strain history of 2024 aluminum alloy, the strain reduction rate of FMLs in the cooling stage is significantly lower than that of 2024 aluminum alloy. This is because the thermal expansion coefficient of the T800/X850 composite after curing is negative. The temperature drop causes the composite to expand. The composite material transforms this expansion into tensile stress applied to the aluminum alloy layer through the interface, so that the rate of strain reduction of the 2024 aluminum alloy in the cooling stage is slowed down. There is a sharp rise in the stress-strain data near the end point. Because the load from the mold and the vacuum bag no longer applied to the part. The tensile stress of metal layer suddenly increased. The monitoring results of three groups is shown in Figure 8 and Figure 9.

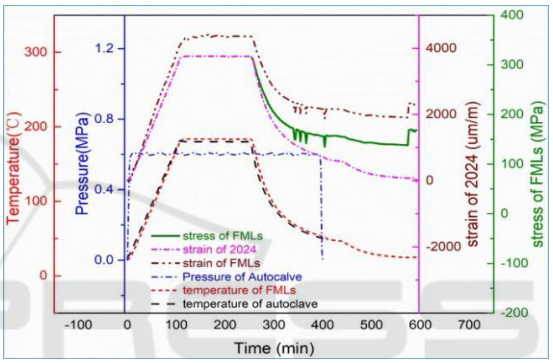

Figure 7: The monitoring results of Group 1 using FBG+TC method.

The internal stress of the metal layer at the end of the cooling of the FMLs is σ_{fbg} =173.307MPa.

The stress results of the FMLs curing process obtained by the three methods are numerically close overall. If the calculation result of the process model is true, the relative errors of the values obtained by the FBG+TC method and the strain definition method are 4.616% and 5.170%, respectively, and the error of the FBG+TC method relative to the "definition method" is 0.5295%. It is evident that the results of the two experimental values are closer. This is because the strain measured of FMLs is determined by many factors, while the theoretical model only considers the most important factors of thermal expansion coefficient mismatch. In another experiment, the asymmetrically laminated parts were solidified and then reheated to a process temperature of 180 °C. It was found that the asymmetrical plates warped at normal temperature were substantially flattened, and the warpage substantially disappeared. The literature (Oken and June, 1895) also shows that the thermal expansion coefficient mismatch is the

main factor contributing to the curing stress of FMLs, so this paper does not consider the effect of curing shrinkage on the curing strain.

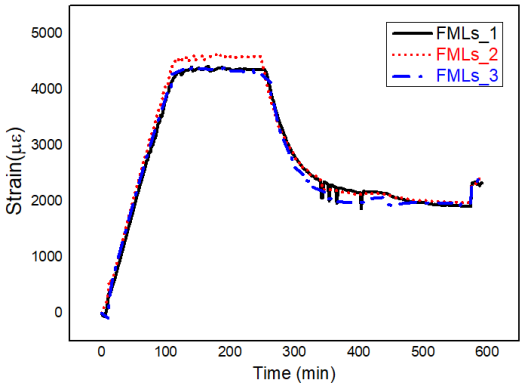

Figure 8: The 3 groups results of FBG+TC method.

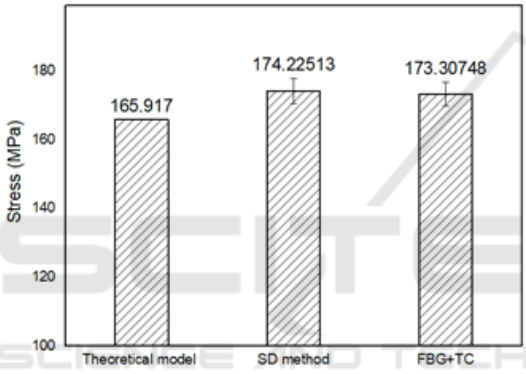

Figure 9: The monitoring results of three methods.

4 CONCLUSIONS

Based on FBG and thermocouple, a strain measurement method suitable for complex process environment is proposed and applied to the monitoring of FMLs autoclave forming process. The strain and temperature of the part are obviously positively correlated. During the cooling process, the metal layer is subject to tensile stress, while the composite layer is to compressive stress. The tensile stress of the metal layer is imposed by the composite layer, and the compressive stress of the composite layer is by the metal layer. Strain measurement methods based on strain definition were proposed, and experiments were carried out. The monitoring results are close to the FBG+TC monitoring results. Since the theoretical model only considers the main factors of thermal expansion coefficient mismatch, but ignores other secondary factors, the model calculation results deviate significantly from the FBG+TC detection results. In general, the FBG+TC method is suitable for the monitoring of the strain during the curing process of FMLs composite parts because it can be used normally in the autoclave process environment and its damage to the measured parts is very small. The definition method is suitable for measuring the strain value at a certain moment and the process model also needs to take more influencing factors into consideration.

ACKNOWLEDGEMENTS

The authors are grateful to the Central South University Graduate Research Innovation Project (1053320171669) and The National Natural Science Foundation of China (No.51675538) for supporting this work.

REFERENCES

Abouhamzeh M., Sinke J., Jansen K. M. B., et al., 2015. Closed form expression for residual stresses and warpage during cure of composite laminates [J]. *Composite Structures*, 133:902-910.

Aniket S., Ratnakar K. and Ashok M., 2016. Review: Fiber Metal Laminates (FML's) - Manufacturing, Test methods and Numerical modeling methods and Numerical modeling [J]. *INTERNATIONAL JOURNAL OF ENGINEERING TECHNOLOGY AND SCIENCES (IJETS)*, 6(1):71-84

Asundi A. and Choi A. Y. N., 1997. Fiber metal laminates: An advanced material for future aircraft [J]. *Journal of Materials Processing Technology*, 63(1–3):384-394.

Botelho E. C., Silva R. A., Pardini L. C., et al., 2006. A review on the development and properties of continuous fiber/epoxy/aluminum hybrid composites for aircraft structures [J]. *Materials Research*, 9(3):247-256.

Dewynter-Marty V., Ferdinand P., Bocherens E., et al. 1998. Embedded Fiber Bragg Grating Sensors for Industrial Composite Cure Monitoring [J]. *Journal of Intelligent Material Systems & Structures*, 9(10):785-787.

Farahi F., Webb D. J., Jones J. D. C., et al., 1990. Simultaneous measurement of temperature and strain: cross-sensitivity considerations [J]. *Journal of Lightwave Technology*, 8(2):138-142.

Ghasemi A. R., Mohammadi M. M., 2016. Residual stress measurement of fiber metal laminates using incremental hole-drilling technique in consideration of the integral method [J]. *International Journal of Mechanical Sciences*, 114:246-256.

Huang S., 1998. Continuous Arbitrary Strain Profile Measurements with Fiber Bragg Gratings [J]. *Smart Materials & Structures*, 7(2):248.

Lo Y. L., Xiao F. Y., 1998. Measurement of corrosion and temperature using a single-pitch Bragg grating fiber sensor [J]. *Journal of Intelligent Material Systems & Structures*, 9(10):800-807.

Majumder M., Gangopadhyay T. K., Chakraborty A. K. et al., 2008. Fibre Bragg gratings in structural health monitoring—Present status and applications [J]. *Sensors & Actuators A Physical*, 147(1):150-164.

Miao H. Y., Demers D., Larose S., et al., 2010. Experimental study of shot peening and stress peen forming [J]. *Journal of Materials Processing Tech*, 210(15):2089-2102.

Moussavi-Torshizi S. E., Dariushi S., Sadighi M., et al., 2010. A study on tensile properties of a novel fiber/metal laminates [J]. *Materials Science & Engineering A*, 527(18-19):4920-4925.

Oken S., June R., R., 1895. Analytical and Experimental Investigation of Aircraft Metal Structures Reinforced with Filamentary Composites. Phase 1. Concept Development and Feasibility. [M]. *NASA CR*, 1977.

Pan L., Yapici U. A., 2015. Comparative study on mechanical properties of carbon fiber/PEEK composites [J]. *Advanced Composite Materials*, 25(4):359-374.

Qiu W., Cheng X., Luo Y., et al., 2013. Simultaneous Measurement of Temperature and Strain Using a Single Bragg Grating in a Few-Mode Polymer Optical Fiber [J]. *Journal of Lightwave Technology*, 31(14):2419-2425.

Rubiogonzález C., Josétrujillo E., Chávez F., et al., 2016. Low velocity impact response of composites and fiber metal laminates with open holes [J]. *Journal of Composite Materials*, 51(6).

Schapery R. A., 1968. Thermal Expansion Coefficients of Composite Materials Based on Energy Principles [J]. *Composite Materials*, 2(3):380-404.

Sexton A., Cantwell W. and Kalyanasundaram S., 2012. Stretch forming studies on a fibre metal laminate based on a self-reinforcing polypropylene composite[J]. *Composite Structures*, 94(2):431-437.

Sinmazçelik T., Avcu E., Bora M. Ö. et al., 2011. A review: Fibre metal laminates, background, bonding types and applied test methods [J]. *Materials & Design*, 32(7): 3671-3685.

Tsartsaris N., Meo M., Dolce F., et al., 2011. Low-velocity impact behavior of fiber metal laminates [J]. *Journal of Composite Materials*, 45(7):803-814.

Vlot A. and Gunnink J. W., 2001. *Fibre Metal Laminates* [M]. Springer Netherlands.

Vlot A., 1996. Impact loading on fibre metal laminates [J]. *International Journal of Impact Engineering*, 18(3):291-307.

Vlot A., 2001. *Glare: history of the development of a new aircraft material* [J]. Springer Netherlands.

Vo T. P., Guan Z. W., Cantwell W. J. et al., 2013. Modelling of the low-impulse blast behavior of fibre–metal laminates based on different aluminum alloys [J]. *Composites Part B Engineering*, 44(1):141-151.

Vogelesang L. B., Vlot A., 2000. Development of fibre metal laminates for advanced aerospace structures [J]. *Journal of Materials Processing Technology*, 103(1):1-5.

Zhang H., Zhang Z., Friedrich K., et al., 2006. Property improvements of in situ epoxy nanocomposites with reduced interparticle distance at high nanosilica content [J]. *Acta Materialia*, 54(7):1833-1842.

Zhu S., Wang Y., Tong M., et al., 2014. Numerical simulation of bird impact on fibre metal laminates [J]. *Polymers & Polymer Composites*, 22(2):147-156.